UNIVERSIDAD NACIONAL DE COLOMBIA
SEDE MEDELLÍN
FACULTAD DE MINAS

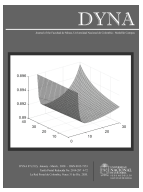

DYNA
http://dyna.medellin.unal.edu.co/

Immobilization of DNA probes on a high frequency piezoelectric biosensor

Camilo Ortiz-Monsalve, Jorge Mario Guerra-González & Marisol Jaramillo-Grajales [b]

[a] *Grupo de Investigación en Ingeniería Biomédica EIA-GIBEC, Universidad EIA, Medellín, Colombia. camilo.ortiz@eia.edu.co, jorge.guerra@eia.edu.co*
[c] *Universidad EIA, Medellin Colombia. marisol.jaramillo@eia.edu.co*

Received: September 17th, 2019. Received in revised form: December 4th, 2019. Accepted: January 21th, 2020

Abstract
In recent years, researchers have taken to biosensors as effective tools for detection due to their portability, low-cost, fast response, and practicality. Piezoelectricity gave way to quartz crystal microbalances (QCM), of which high-frequency QCMs (HFF-QCM 100MHz) are still being researched. In this paper, we use DNA immobilization on a HFF-QCM via self-assembled monolayers (SAM) technique. Immobilization was initially verified with ATR-FTIR. Then, DNA was immobilized in real time on the HFF-QCM crystals. A variation in the phase of the signal suggests fixation of DNA to the surface, in accordance with ATR-FTIR results. A density of 629 ng/cm^2 was computed. Also, a positive correlation between immobilized DNA and DNA concentration, and the appearance of a saturation point between 1 and 5 μM were shown after analysis of different DNA concentrations.

Keywords: DNA; self-assembled monolayers; SAM; biosensors; quartz crystal microbalances, QCM; high-frequency, HFF-QCM; genosensor.

Inmovilización de sondas de ADN en un biosensor de alta frecuencia

Resumen
En los últimos años, el interés en los biosensores ha aumentado ya que son efectivos, pueden ser portables y de bajo costo, tienen respuesta rápida y son de fácil uso. El fenómeno piezoeléctrico dio lugar a microbalanzas de cristal de cuarzo (QCM); QCM de alta frecuencia (HFF-QCM 100MHz) su comportamiento característico aún está en investigación. Se analizó la inmovilización de ADN para HFF-QCM. La inmovilización de ADN conjugado en cristales de cuarzo recubiertos de oro se realizó mediante monocapas autoensambladas (SAM). Luego, el ADN se inmovilizó en tiempo real en el HFF-QCM en cristales. La variación en la fase de la señal sugiere que el ADN se fijó efectivamente a la superficie, lo que es consistente con los resultados de ATR-FTIR. Se calculó una densidad de 629 ng /cm^2. Finalmente, el análisis de diferentes concentraciones de ADN en tiempo real, muestra una correlación positiva entre el ADN inmovilizado y la concentración de ADN, y la aparición de un punto de saturación entre 1 y 5 μM.

Palabras clave: ADN; monocapas autoensambladas; biosensores; microbalanza de cristal de cuarzo; alta frecuencia; genosensor.

1. Introduction

Fast monitoring of biological events improves quality control processes, makes medical diagnoses faster and more accurate, and expedites laboratory testing and bioprocess innovation. Biosensor technologies combine the ability of electronics to read and process signals with the specificity and sensitivity of biological systems. They are acknowledged as effective detection tools due to their portability, low-cost, fast response, practicality, and minimal sample preparation requirements, unlike traditional analytical methods [1,2].

Piezoelectric materials accumulate electric potential when stressed; alternating voltage makes them oscillate at their resonant frequency [3]. Quartz crystal microbalances (QCM), one of such, are widely used in small mass detection and can effectively transform changes in mass into measure

How to cite: Ortiz-Monsalve, C, Guerra-González, J.M, and Jaramillo-Grajales, M, Immobilization of DNA Probes on a High Frequency Piezoelectric Biosensor. DYNA, 87(212), pp. 163-168, January - March, 2020.

shifts in frequency. This relationship between frequency and mass was first described by Sauerbrey in 1959, as shown in Equation 1, where A_p represents the area, μ_p the shear modulus, ρ_p the density, and f_o the natural frequency of crystal [4].

$$\Delta f = -\frac{2 f_0^2}{A_p \sqrt{\mu_p \rho_p}} \Delta m = -K \Delta m \quad (1)$$

A typical piezoelectric quartz crystal consists of a thin piece of compressed, gold-coated quartz. A holder is required for manipulation. The most frequently used QCMs operate in frequencies ranging from 5MHz through 20MHz [3], although high fundamental frequency crystals (HFF-QCM), which are more sensitive, are also available. Unlike other systems, HFF-QCMs do not produce a shift in frequency after a change in mass density has been detected on the surface. Instead, they produce a shift in signal phase [5]. The relationship between mass and signal phase is shown in eq. 2, where $\Delta\varphi$ represents the phase shift, Δm_s represents the change in mass density, and m_L represents the effect of the liquid displaced by the crystal.

$$\Delta\varphi \approx -\frac{\Delta m_s}{m_L} \quad (2)$$

According to the biological event being monitored, one can use either enzymatic biosensors, microbial biosensors, or immunosensors [1]. A genosensor or "DNA biosensor" is a new type of tool that uses DNA probes to identify specific DNA-DNA bonds [6]. Typical applications of these include pathogen identification, monitoring of gene expression, diagnosis of genetic disorders, and many other applications in the pharmaceutical and forensic sciences [7]. The most advanced DNA biosensors make use of optical techniques, although piezoelectric and acoustic devices have shown equal performance at significantly lower cost [3,8].

Biosensors consist of a transducer bound to an immobilized biological interface. Immobilization must be intimate and stable, which determines the quality of the detection signal and the reusability of the sensor [9]. Self-assembled monolayers (SAM), which are arrays of thiol-based molecules, are widely used in bioreceptor immobilization, due to their high affinity to gold surfaces [10]. These have a terminal group that can vary according to the biomolecule of interest (proteins, nucleic acids, etc.) [11]. Occasionally, inactive molecules are added in to control molecule distribution and enable bioreceptor-analyte interaction; these arrays are known as mixed-SAM (MSAM) [12,13].

When assembling a genosensor, single-stranded DNA is directly immobilized on the surface of gold by adding a thiol group (usually through phosphonamidites bond formation) [7]. This process is simple and fast but easily influenced by the physisorption of the chain on the surface of gold [14]. On the other hand, conjugated single-stranded DNA can be indirectly linked to the surface via SAM/MSAM. This technique is slightly more complex but increases ssDNA exposure to the complementary chain. In such case, 1-Ethyl-3 (-3 dimethyl-amino-propyl) carbodiimide hydrochloride (EDC) and N-hydroxy succinimide (NHS) can contribute to the activation and stabilization of the bond [7].

In this research, we developed a bioreceptor by immobilizing ssDNA on alkanethiol SAM over a gold surface. This bioreceptor was later used on HFF-QCM genosensors.

2. Materials and methods

2.1. Reagents and equipment

Freeze-dried and HPLC-purified single-stranded DNA (5'-T_{15}AATGTGTGCAATATTAATTACAAGTGTG-3') was acquired from Invitrogen. EDC and NHS, stored at -20°C and 4°C, respectively, were acquired from Thermoscientific. Ethylenediamide (EA) and ethanol, stored at room temperature, were acquired from Panreac. Acetic acid (AA) and sodium acetate (SA) were acquired from Merck. 16-mercaptohexadecanoic acid (MHDA) and 11-mercaptoundecanol (MUA) were acquired from SigmaAldrich and stored at 4 and -20 °C, respectively.

Water was purified using a Synergy UV system by Millipore, and the concentration of DNA was measured in a NanoDrop 2000 spectrophotometer (Thermoscientific). Infrared spectra was obtained from a FTIR spectrophotometer (Spectrum 100) with an Attenuated Total Reflectance (ATR- FTIR) accessory by PerkinElmer. UV/Ozone ProCleaner Plus was acquired from Bioforce.

The 10 MHz and 100 MHz QCMs were purchased from AWSensors. An AWS A20 system and A20RP software by AWSensors were used for signal monitoring. The main microfluidic pump was acquired from Labotaq and a secondary pump from Cole-Parmer.

2.2. Procedures

2.2.1. Chemical DNA Conjugation

DNA was conjugated using phosphoramidite bond formation, as described by Hermanson [15] This process was carried out at the Biotechnology Laboratory at Universidad CES, Colombia. First, 5 µl of 0.1 M buffer acetate (pH 4.5), 0.1 µl of 3 M ethanolamine, 33.3 µl of 200 µM ssDNA, 0.6 mg of NHS, and 4.9 mg of EDC were mixed into a 2 ml vial and left to set for 2 hours. Then, the solution was transferred to a new vial, and 150 µl of ultrapure water, 20 µl of 3 M sodium acetate, and 400 µl of absolute ethanol (-20 °C) were added into. The solution was homogenized and stored overnight at -20 °C to allow incubation. Finally, it was centrifuged for 30 minutes at 4 °C. At this point, a DNA pellet was easily identifiable. The supernatant was carefully discarded, and the pellet was washed with a 95% ethanol solution, let dry, and the remainder was suspended in 100 µl of ultrapure water. Soon after, the concentration of ss-DNA solution was checked in a *Nanodrop 2000* spectrophotometer.

2.2.2. Immobilization of DNA on the gold surfaces.

Immobilization on the 100MHz QCM

The crystals were rinsed with water and ethanol, and then dried with nitrogen gas for cleaning. Then, they were introduced in a UV/Ozone ProCleaner for 20 minutes, rinsed and dried again.

For MSAM formation, a 250 µM alkanethiol solution was prepared, MHDA:MUA (1:25). This specific proportions can be used with DNA[16]. The crystals were left overnight in 500 µl of the solution, at room temperature with magnetic agitation The next day, these were rinsed with ethanol and dried with nitrogen gas. To activate the monolayers, the crystals were placed in an immobilization chamber for 4 hours with 500 µl of an activating solution consisting of 200 mM EDC, and 50 mM NHS. Then, they were rinsed with ethanol and dried again using nitrogen gas.

DNA was immobilized on the activated surface, and a 100 MHz sensing system was used to monitor the adherence of conjugated DNA on the MSAM. Milli-Q water was used to find a baseline, and then, DNA samples were injected at a flow rate of 20 µl/min. To verify the sensitivity of the biosensor and the effectiveness of DNA immobilization, samples were injected at concentrations of 5 µM, 1 µM, and 0.1 uM.

Immobilization on the 10 MHz QCM

Due to the fragility of the QCMs, the 100 MHz interfaces using could not be characterized using the techniques we had available. For that reason, we used coarser 10 MHz interfaces to perform the characterization experiments.

The same immobilization process was performed on the new QCMs, with a few minor modifications: In addition to the UV/Ozone cleaning process, we used an extra cleaning step by immersing the crystals in piranha-etch (H_2O_2 + H_2SO_4 (1:3)) for 5 min; SAM were then formed using a 10mM MHDA alkanethiol solution. The surface of the crystal was examined with ATR-FTIR using a resolution of 4 cm^{-1} and 20 scans.

3. Results

3.1. FTIR

The success of the immobilization process was verified across all stages using ATR-FTIR. Initially, we evaluated the formation of SAM, followed by their activation, and the posterior immobilization of DNA. In Fig. 1, peaks appear on the spectra at 2856 cm^{-1} and 2928 cm^{-1} after SAM immobilization. These bands are attributed to the symmetrical and asymmetrical vibrations of CH_2 and suggest the formation of SAM on the surface of gold. The appearance of troughs on these bands has been reported extensively [17]. Himmelhaus *et al.* reported shifting of bands across the spectra, from 2813 cm^{-1} to 2851 cm^{-1}, and from 2916 cm^{-1} to 2919 cm^{-1}, indicating SAM formation [18]. Also, Marshall *et al.* evaluated the adsorption of alkanethiols of varied chain length on GaAs (001), confirming how it is possible to determine the degree of imperfections on the SAM via analysis of the spectra between 2800 cm^{-1} and 3000 cm^{-1} [19].

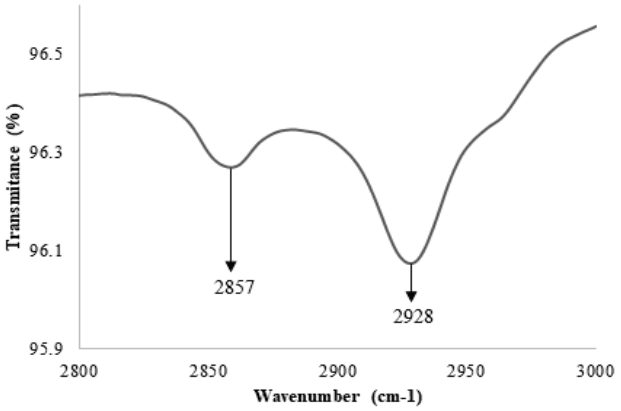

Figure 1. Formation of SAM on the surface of gold. The bands at 2857 cm^{-1} and 2928 cm^{-1} are characteristic of the carbon skeleton structure.
Source: The Authors.

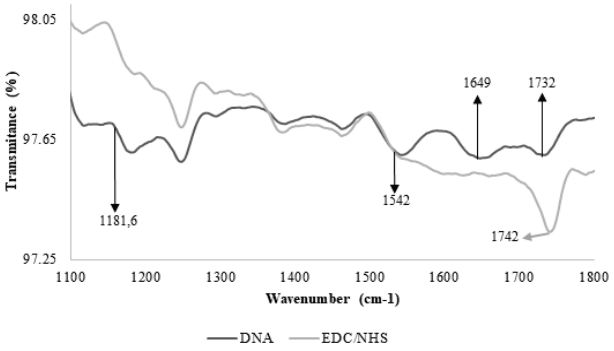

Figure 2. Transmittance spectra from the surface of gold-coated crystals. Two stages are observed: 1) The activation of SAM, indicated by the appearance of a trough around 1742 cm^{-1}, and 2) The immobilization of DNA, indicated by the appearance of troughs around 1542 cm^{-1} and 1649 cm^{-1}.
Source: The Authors.

Fig. 2 shows the most important bands after activation of SAM and immobilization of DNA. The image shows the progression, which occurred in similar fashion to Bhadra *et al*'s, when they immobilized proteins on the surface of gold [20]. After activation, a trough appears at 1745 cm^{-1}, attributed to the ester group in NHS.

It has been suggested before that the formation of an ester leads to the appearance of troughs around 1818 cm^{-1}, 1784 cm^{-1} and 1743 cm^{-1} [21][22], but given the natural frequency of the ATR tool crystal we used, it was impossible to detect anything on the bands ranging from 1800 cm^{-1} to 2600 cm^{-1}. As such, we only report a trough at 1745 cm^{-1}, which we expect is attributed to the formation of an ester group (as it does not appear before SAM activation).

Finally, after DNA immobilization, two more troughs appeared around 1540 cm^{-1} and 1650 cm^{-1}. These findings are consistent with Sun *et al's*, who, using the same methods, reported troughs around 1552 cm^{-1} and 1662 cm^{-1}, and attributed them to the extension of the carbon skeleton

structure and the DNA bases, respectively [23].

Overall, bands in this range have been attributed to the carbonyl group of chemisorbed thymines [24] and to the vibration of the double bond in nitrogenous bases [25]. In addition, bands corresponding to the ring-like structure of purines at 1464 cm^{-1}, and of pyrimidines at 1525 cm^{-1} have also been reported, as well as those for C=O bonds (at 1600 cm^{-1}) and C=N bonds (at 1750 cm^{-1}) [26]. Based on these findings, we confirm the immobilization of DNA on the surface of gold.

3.2. Real time immobilization of DNA on the 100 MHz crystals

Fig. 3 shows the results after immobilization of 1 µM DNA on the surface of the 100 MHz crystal. Initially, a baseline period is observed, which corresponds to the flow of Milli-Q water over the activated crystal. During this period, no immobilization of molecules on the surface of the crystal occurs and as such, no shift in the phase of the signal is observed. After injection of 250 µl of DNA, a reduction of approximately 375 mV is observed. Finally, when the sample stops flowing over the crystal, water resumes, and baseline is shown again.

The variation in the phase of the signal suggests DNA was effectively fixed to the surface, which is consistent with the ATR-FTIR results. The shift in phase occurred in two stages: 1) an initial descent, followed by the stabilization of the signal, and 2) a final descent followed by reappearance of the baseline. This trend is owed to the viscous effect of DNA flowing over the surface of the crystal, but it is only through comparison of the initial and final baselines that the amount of DNA on the surface can be determined. The viscous effect has been reported by other authors who used different QCMs [27]. We have not found other studies reporting the use of high fundamental frequency quartz crystal microbalances (HFF-QCM) to evaluate the immobilization of DNA, although some authors have evaluated its immobilization on QCMs: Kupciunate et al. studied the immobilization of ssDNA on the surface of gold and its posterior hybridization using a QCM and 10 MHz crystals [14]. In their paper, they showed how a change in frequency confirms immobilization of DNA and computed a surface density of 629 ng/cm^2. In comparison, the density we calculated was 10.52 pg/mm^2, which is much larger. We expect the difference in ours to be associated to variations in the experimental setup and the increased sensitivity of our HFF-QCM. Thus, the results here shown represent a valuable contribution to the understanding of these tools.

Finally, we measured the effect of varied concentrations of DNA on the biosensor's response, and indirectly computed the amount of DNA immobilized on the surface. Fig. 4 shows the signals obtained. For the evaluated concentrations (0.1, 1 and 5 µM), we observed a similar behavior in the signal, which presents an initial baseline period and a phase shift when the sample touches the crystal. We also found that the magnitude of the phase shift is directly proportional to the concentration used (approximately 65, 375 and 350 mV respectively), but, with concentrations of 1 µM and 5 µM, the changes obtained were very similar, indicating a proximity to a zone of saturation. Analogously, we computed the surface density for each concentration and found values of 1.82, 10.52 and 9.81 pg/mm^2, respectively.

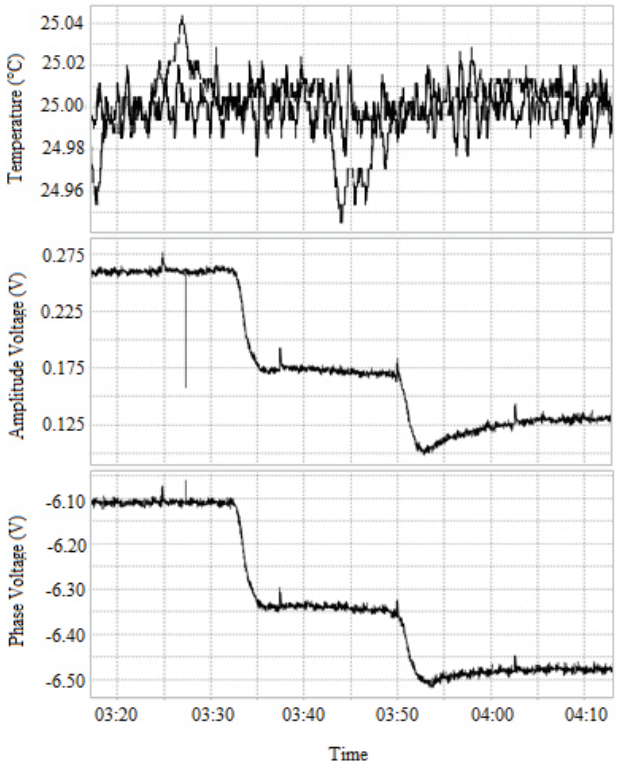

Figure 3. Response of the HFF-QCM to the immobilization of 1 µM DNA. The signal phase response (bottom) shows an initial baseline period. Once the sample touches the surface of the crystal, there is a variation in the signal phase.
Source: The Authors.

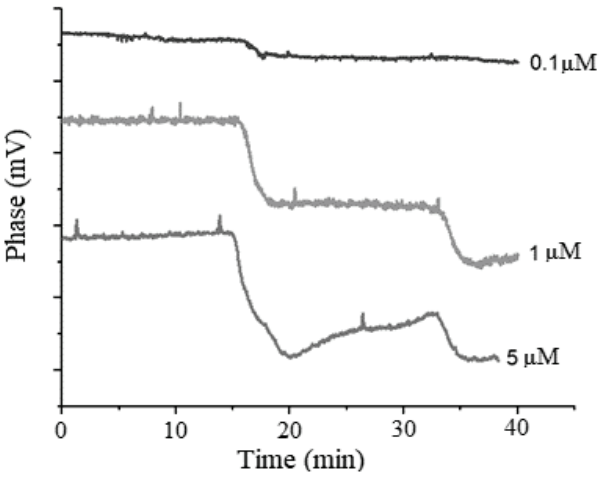

Figure 4. Response of the HFF-QCM to the variation in the concentration of immobilized DNA. The increase in concentration is consistent with an increase in phase shift. Concentrations of 1 µM and 5 µM show a similar change in magnitude, compared to 0.1µM test, which suggests saturation.
Source: The Authors.

4. Conclusions

The indirect immobilization of conjugated DNA on the gold-coated quartz crystals was confirmed by ATR-FTIR spectroscopy. The appearance of bands after each stage proves SAM formation, carboxyl-group activation, and DNA immobilization. In addition, the HFF-QCM also confirmed the immobilization of DNA on the 100 MHz crystals. The phase shift observed was related to a mass change on the surface of the crystal, confirming immobilization of DNA on the surface. Finally, analyses of different concentrations of DNA show a positive correlation between immobilized DNA and DNA concentration, and the appearance of a saturation point between 1 and 5 μM.

Although the method we used here does not distinguish chemisorbed DNA from physisorbed DNA, we do plan to address DNA hybridization at some point in the future.

Acknowledgments

The authors would like to extend their gratitude to Universidad EIA for all the support provided.

References

[1] Pacheco, J.G., Barroso, M.F., Nouws, H.P.A., Morais, S. and Delerue-Matos, C. Biosensors, in: Curr. Dev. Biotechnol. Bioeng., Elsevier, 2017, pp. 627-648. DOI: 10.1016/B978-0-444-63663-8.00021-5.

[2] Jha, S.N., Biosensor, in: Rapid Detect. Food Adulterants Contam., Elsevier, 2016, pp. 125-145. DOI: 10.1016/B978-0-12-420084-5.00005-6.

[3] Evtugyn, G.A., Biosensors for pesticides and foodborne pathogens, in: Portable Biosensing Food Toxicants Environ. Pollut., CRC Press, 2013, pp. 605-679. DOI: 10.1201/b15589.

[4] Sauerbrey, G., Verwendung von schwingquarzen zur wägung dünner schichten und zur mikrowägung. Zeitschrift Für Phys. 155(2), pp. 206-222, 1959. DOI: 10.1007/BF01337937.

[5] Montagut-Ferizzola, Y.J., Sistema oscilador mejorado para aplicaciones de microbalanza (QCM) en medios líquidos y propuesta de un nuevo método de caracterización para biosensores piezoeléctricos, PhD. Thesis, Departament d'Enginyeria Electrònica, Universitat Politècnica de València, España, 2011. DOI: 10.4995/Thesis/10251/9688.

[6] Oliveira-Brett, A.M., Diculescu, V.C., Chiorcea-Paquim, A.M. and Serrano, S.H.P., Chapter 20 DNA-electrochemical biosensors for investigating DNA damage. Compr. Anal. Chem., 49, pp. 413-437, 2007. DOI: 10.1016/S0166-526X(06)49020-6.

[7] García-Carrascosa, L., Desarrollo de un multibiosensor de ADN para el diagnóstico temprano de cáncer de mama, PhD. Thesis, Departamento de Biología Molecular de la Facultad de Ciencias de la Universidad Autónoma de Madrid, España, 2008.

[8] Lavrik, N.V., Sepaniak, M.J. and Datskos, P.G., Cantilever transducers as a platform for chemical and biological sensors. Rev. Sci. Instrum. 75, pp. 2229-2253, 2004. DOI: 10.1063/1.1763252.

[9] Su, L., Jia, W., Hou, C. and Lei, Y., Microbial biosensors: a review. Biosens. Bioelectron. 26, pp. 1788-1799, 2011. DOI: 10.1016/j.bios.2010.09.005.

[10] Park, C.S., Colorado, R., Jamison, A.C. and Lee, T.R., Thiol-based self-assembled monolayers: formation, organization, and the role of adsorbate structure, in: Ref. Modul. Mater. Sci. Mater. Eng., Elsevier, 2016. DOI: 10.1016/b978-0-12-803581-8.03780-2.

[11] Schreiber, F., Structure and growth of self-assembling monolayers. Prog. Surf. Sci. 65, pp. 151-256, 2000. DOI: 10.1016/S0079-6816(00)00024-1.

[12] Ocampo, A., Jaramillo, M., March, C. and Montoya, Á., Inmunosensor piezoeléctrico para la detección del metabolito 3,5,6-tricloro-2-piridinol del plaguicida clorpirifos. Rev. EIA. 16, pp. 127-136, 2011.

[13] Vericat, C., Vela, M.E., Benitez, G., Carro, P. and Salvarezza, R.C., Self-assembled monolayers of thiols and dithiols on gold: new challenges for a well-known system. Chem. Soc. Rev. 25(2), pp. 1805-1834, 2010. DOI: 10.1039/b907301a.

[14] Tombelli, S., Minunni, M., Santucci, A., Spiriti, M.M. and Mascini, M., A DNA-based piezoelectric biosensor: strategies for coupling nucleic acids to piezoelectric devices. Talanta. 68(3), pp. 806-812, 2006. DOI: 10.1016/j.talanta.2005.06.007.

[15] Hermanson, G.T., Nucleic acid and oligonucleotide modification and conjugation, in Bioconjugate Techniques, Elsevier, 2013, pp. 959-987.DOI: 10.1016/b978-0-12-382239-0.00023-6.

[16] Naturwissenschaften, D.D., Optimization of interfaces for genosensors based on thiol layers on gold films, PhD. dissertation, Fakultat IV Chemie und Pharmazie, Universitat Regensburg, Germany, 2001.

[17] Sam, S., Touahir, L., Salvador-Andresa, J., Allongue, P., Chazalviel, J.N., Gouget-Laemmel, A.C., De Villeneuve, C.H., Moraillon, A., Ozanam, F., Gabouze, N. and Djebbar, S., Semiquantitative study of the EDC/NHS activation of acid terminal groups at modified porous silicon surfaces. Langmuir. 26(2), pp. 809-814, 2010. DOI: 10.1021/la902220a.

[18] Himmelhaus, M., Eisert, F., Buck, M. and Grunze, M., Self-assembly of n-alkanethiol monolayers. A study by IR-visible sum frequency spectroscopy (SFG). J. Phys. Chem. B. 104(3), pp. 576-584, 2000. DOI: 10.1021/Jp992073e.

[19] Marshall, G.M., Bensebaa, F. and Dubowski, J.J., Observation of surface enhanced IR absorption coefficient in alkanethiol based self-assembled monolayers on GaAs(001). J. Appl. Phys. 105(9), pp.1-7, 2009. DOI: 10.1063/1.3122052.

[20] Bhadra, P., Shajahan, M.S., Bhattacharya, E. and Chadha, A., Studies on varying n-alkanethiol chain lengths on a gold coated surface and their effect on antibody-antigen binding efficiency. RSC Adv. 5(98), pp.80480-80487, 2015. DOI: 10.1039/c5ra11725a.

[21] Palazon, F., Montenegro-Benavides, C., Léonard, D., Souteyrand, E. Chevolot, Y. and Cloarec, J., Supporting information for : Carbodiimide / NHS derivatization of COOH-terminated SAMs : activation or byproduct formation?. Langmuir. 30(16), pp.4545-50, 2014. DOI: 10.1021/la5004269.

[22] Yan, Q., Zheng, H.N., Jiang, C., Li, K. and Xiao, S.J., EDC/NHS activation mechanism of polymethacrylic acid: anhydride versus NHS-ester. RSC Adv. 5(86), pp.69939-69947, 2015. DOI: 10.1039/c5ra13844b.

[23] Sun, X., He, P., Liu, S., Ye, J. and Fang, Y., Immobilization of single-stranded deoxyribonucleic acid on gold electrode with self-assembled aminoethanethiol monolayer for dna electrochemical sensor applications. Talanta. 47(2), pp. 487-495, 1998. DOI: 10.1016/S0039-9140(98)00108-8.

[24] Petrovykh, D.Y., Kimura-Suda, H., Whitman, L.J. and Tarlov, M.J., Quantitative analysis and characterization of DNA immobilized on gold. J. Am. Chem. Soc. 125(17), pp. 5219-5226, 2003. DOI: 10.1021/ja029450c.

[25] Boncheva, M., Scheibler, L., Lincoln, P., Vogel, H. and Åkerman, B., Design of oligonucleotide arrays at interfaces. Langmuir. 15(13), pp.4317-4320, 1999. DOI: 10.1021/la981702t.

[26] Kumar, K.S. and Naaman, R., Quantitative analysis and characterization of self- assembled DNA on a silver surface. Langmuir. 28(41), pp.14514-14517, 2012. DOI: 10.1021/la302999t.

[27] Thourson, S.B., Marsh, C., Doyle, B.J. and Timpe, S.J., Quartz crystal microbalance study of bovine serum albumin adsorption onto self-assembled monolayer-functionalized gold with subsequent ligand binding. Colloids Surfaces B Biointerfaces, 111, pp.707-712, 2013. DOI: 10.1016/j.colsurfb.2013.06.053.

C. Ortiz-Monsalve, completed his BSc. in Chemical Engineering in 2016 from the Universidad Nacional de Colombia, Medellin, Colombia, and a BSc. in Biomedical Engineering at Universidad EIA, Medellin, Colombia. Currently, he is studying a MSc. in Biofabrication at Universität Bayreuth, Bayreuth, Germany. From 2016 to 2018, he worked in biosensors research studying immobilization of DNA and proteins on a surface.

ORCID: 0000-0002-9523-2773

J.M. Guerra-González completed his BSc in Biomedical Engineering from the EIA University in 2016 and is currently pursuing a MSc. in Biomedical Computing at Technische Universität München, Germany. A former intern of the faculty's laboratory, Jorge has contributed to developing methodologies for DNA immobilization for their application in high frequency biosensors. Currently, he is actively involved in medical data science research using artificial intelligence for automatic liver lesion segmentation.
ORCID: 0000-0002-6075-8644

M. Jaramillo-Grajales, completed her BSc in Chemical Engineering in 2000, her MSc. in Biotecnology in 2005, and her PhD in Biotecnology in 2016, all of them from the Universidad Nacional de Colombia. Medellín, Colombia. She is a current professor of biological sciences at Universidad EIA, where she leads the biomedical engineering research group GIBEC. Her research involves developing new technologies to detect and obtain biomarkers. She has supervised projects that aim to develop new biosensors via surface modification techniques that employ proteins and DNA.
ORCID: 0000-0003-1907-6614